

# UC Irvine

## UC Irvine Previously Published Works

### Title

Pygo2 regulates  $\beta$ -catenin-induced activation of hair follicle stem/progenitor cells and skin hyperplasia

### Permalink

<https://escholarship.org/uc/item/1w1221xw>

### Journal

Proceedings of the National Academy of Sciences of the United States of America, 111(28)

### ISSN

0027-8424

### Authors

Sun, Peng  
Watanabe, Kazuhide  
Fallahi, Magid  
et al.

### Publication Date

2014-07-15

### DOI

10.1073/pnas.1311395111

### Copyright Information

This work is made available under the terms of a Creative Commons Attribution License, available at <https://creativecommons.org/licenses/by/4.0/>

Peer reviewed

# Pygo2 regulates $\beta$ -catenin–induced activation of hair follicle stem/progenitor cells and skin hyperplasia

Peng Sun<sup>a,1</sup>, Kazuhide Watanabe<sup>a,1</sup>, Magid Fallahi<sup>a</sup>, Briana Lee<sup>a</sup>, Megan E. Afetian<sup>a</sup>, Catherine Rheume<sup>a</sup>, Di Wu<sup>a</sup>, Valerie Horsley<sup>b</sup>, and Xing Dai<sup>a,2</sup>

<sup>a</sup>Department of Biological Chemistry, School of Medicine, University of California, Irvine, CA 92697; and <sup>b</sup>Departments of Molecular, Cellular and Developmental Biology and Dermatology, Yale University, New Haven, CT 06520

Edited by Elaine Fuchs, The Rockefeller University, New York, NY, and approved June 4, 2014 (received for review June 18, 2013)

**Understanding the epigenetic mechanisms that control the activation of adult stem cells holds the promise of tissue and organ regeneration. Hair follicle stem cells have emerged as a prime model to study stem cell activation. Wnt/ $\beta$ -catenin signaling controls multiple aspects of skin epithelial regeneration, with its excessive activity promoting the hyperactivation of hair follicle stem/progenitor cells and tumorigenesis. The contribution of chromatin factors in regulating Wnt/ $\beta$ -catenin pathway function in these processes is unknown. Here, we show that chromatin effector Pygopus homolog 2 (Pygo2) produced by the epithelial cells facilitates depilation-induced hair regeneration, as well as  $\beta$ -catenin–induced activation of hair follicle stem/early progenitor cells and trichofolliculoma-like skin hyperplasia. Pygo2 maximizes the expression of Wnt/ $\beta$ -catenin targets, but is dispensable for  $\beta$ -catenin–mediated expansion of LIM/homeobox protein Lhx2<sup>+</sup> cells, in the stem/early progenitor cell compartment of the hair follicle. Moreover,  $\beta$ -catenin and Pygo2 converge to induce the accumulation and acetylation of tumor suppressor protein p53 upon the cell cycle entry of hair follicle early progenitor cells and in cultured keratinocytes. These findings identify Pygo2 as an important regulator of Wnt/ $\beta$ -catenin function in skin epithelia and p53 activation as a prominent downstream event of  $\beta$ -catenin/Pygo2 action in stem cell activation.**

Research in recent years has established the skin as an excellent model to study molecular mechanisms that control regenerative processes. Throughout life, the interfollicular epidermis (IFE) is continuously renewed due to proliferative activity of the basal layer, whereas a hair follicle (HF) undergoes cyclic bouts of growth (anagen), regression (catagen), and resting (telogen) (1). Regeneration of the new HF is fueled by stem cells (SCs) in the bulge and their immediate progeny in the secondary hair germ (HG) (2, 3). Bulge and HG cells are relatively slow cycling during telogen, but become actively proliferative in a sequential manner upon transition into anagen (4). Several molecular pathways that control HF SC/early progenitor cell (EPC) behaviors have been identified and are intimately linked to skin self-renewal, repair, or tumorigenesis (1, 3).

The Wnt/ $\beta$ -catenin signaling pathway is essential for self-renewal and tumorigenesis in myriad tissues (5). Conditional loss of  $\beta$ -catenin globally in skin epithelia leads to SC exhaustion, whereas HF SC/EPC-specific ablation curtails the proliferation of HG progenitor cells and fate specification of bulge SCs without affecting SC maintenance/viability (6–9). Conversely, expression of an N-terminally truncated, nondegradable form of  $\beta$ -catenin ( $\Delta$ N- $\beta$ -catenin or NBC) results in a range of skin phenotypes including premature anagen entry via precocious SC activation, skin hyperplasia characterized by de novo HFs and trichofolliculoma-like overgrowths, and pilomatricomas (4, 8, 10–12). Although transcriptional targets of Wnt/ $\beta$ -catenin signaling in HF SC/EPCs have been identified, the molecular and functional interactions between  $\beta$ -catenin and chromatin regulators that control tissue regeneration in the skin are not well understood.

The Pygopus (Pygo) family of proteins regulates Wnt/ $\beta$ -catenin signaling by controlling transcription (13) as well as linking this pathway to changes in epigenetic chromatin marks. Pygo proteins

directly bind to an active transcriptional histone mark, lysine 4-trimethylated histone H3 (H3K4me3) (14, 15). Furthermore, Pygo2 regulates the production of histone marks at target loci in part by recruiting histone-modifying enzymes (15–20). Germ-line deletion of *Pygo2* results in improper HF morphogenesis (21). However, whether Pygo2 interacts with Wnt/ $\beta$ -catenin signaling to regulate adult HF regeneration is unknown.

Here, we show that conditional deletion of *Pygo2* in the skin epithelium suppresses depilation- and NBC-induced anagen entry, precocious HG proliferation, and follicular hyperplasia. We dissect Pygo2-dependent and -independent effects of NBC and provide evidence for Pygo2-facilitated accumulation and acetylation of p53 upon  $\beta$ -catenin overexpression and/or in activated HG cells. These findings highlight Pygo2 as an important downstream mediator of  $\beta$ -catenin function in regenerative proliferation processes of the skin.

## Results

**Skin Epithelia-Specific Deletion of *Pygo2* Does Not Impact HF Morphogenesis or Postnatal Cycling.** During morphogenesis, *Pygo2* null mice displayed reduced HF density (21), but relatively normal IFE differentiation (Fig. S1). Because Pygo2 protein was detected in both epithelial and stromal components of the developing HF (Fig. S2), we sought to use the *K14-Cre* mice to generate skin epithelia-specific *Pygo2* knockout (SSKO: *K14-Cre/Pygo2*<sup>flxed/-</sup>) to assess the importance of epithelially expressed Pygo2. Despite efficient Cre-mediated deletion (15), SSKO animals showed largely normal epidermal and HF morphogenesis (Fig. S3A).

## Significance

Stem cells in the hair follicle are quiescent when the follicle is resting, but rapidly expand and differentiate upon proper cues to fuel hair regeneration, skin repair, and even cancer formation. Here we identify an important regulator of this activation process, namely Pygopus homolog 2 (Pygo2), a protein that acts in Wnt/ $\beta$ -catenin signaling and has chromatin regulatory activity. When Pygo2 is absent, overactive  $\beta$ -catenin signaling or hair depilation can no longer efficiently induce stem cell activation and follicular regeneration; expression of Wnt/ $\beta$ -catenin target genes decreases, and follicular hyperplasia subsides. Interestingly, Pygo2 works with  $\beta$ -catenin to increase the level and activation of tumor suppressor protein p53. These findings provide important insights into the regulation of skin regeneration and tumorigenesis.

Author contributions: P.S., K.W., V.H., and X.D. designed research; P.S., K.W., M.F., B.L., M.E.A., C.R., and D.W. performed research; P.S., K.W., M.F., B.L., C.R., and X.D. analyzed data; and V.H. and X.D. wrote the paper.

The authors declare no conflict of interest.

This article is a PNAS Direct Submission.

<sup>1</sup>P.S. and K.W. contributed equally to this work.

<sup>2</sup>To whom correspondence should be addressed. E-mail: xdai@uci.edu.

This article contains supporting information online at [www.pnas.org/lookup/suppl/doi:10.1073/pnas.1311395111/-DCSupplemental](http://www.pnas.org/lookup/suppl/doi:10.1073/pnas.1311395111/-DCSupplemental).

A predominant site of *Pygo2* expression in the developing HF is the presumptive bulge where future adult SCs reside (Fig. 1*A* and Fig. S2). In the adult, nuclear *Pygo2* was largely absent from the CD34<sup>+</sup> bulge cells at telogen (Fig. 1*B*), but was detected in the bulge at anagen (Fig. 1*C*). During telogen-to-anagen (T–A) transition, nuclear *Pygo2* began to be expressed in the lower bulge and HG (Fig. 1*D*), coinciding with SC/EPC activation. As anagen progressed, *Pygo2* persisted in a subset of the outer root sheath (ORS), inner root sheath (IRS), cortex precursor cells, as well as in the dermal papillae (DP), but was absent from the transit-amplifying cells in the matrix (Fig. 1*E–G*). Costaining with proliferating cell nuclear antigen (PCNA) revealed a partial overlap between *Pygo2* expression and proliferative activity (Fig. 1*G*, *Inset*; ~50% of the PCNA<sup>+</sup> HG cells express *Pygo2*). These data reveal a dynamic expression of nuclear *Pygo2* in proliferative stem/progenitor cells of the HF.

Despite *Pygo2*'s expression in keratinocytes of adult HF, SSKO mice produced a normal hair coat, unlike the sparse hair coat in two adult *Pygo2*<sup>-/-</sup> mice that escaped perinatal lethality (21) (Fig. S4). Furthermore, histological analysis revealed no obvious hair cycle defects in SSKO mice (Fig. S3). To determine if wound-induced hair regeneration was altered in SSKO mice, we depilated hair at telogen, which induces anagen entry and subsequent hair regeneration (22). Interestingly, depilation elicited a dramatic elevation of *Pygo2* in both HFs and IFE (Fig. 1*H* and *I*), and SSKO mice showed a reproducible delay in the formation of new hairs (Fig. 1*J*). Moreover, a quantitative analysis of the length of the regenerating HFs revealed a statistically significant reduction in the SSKO samples (Fig. 1*K*). Finally, immunostaining for Ki67 revealed a reduced number of proliferative cells in both HFs and IFE of the SSKO skin (Fig. 1*L* and *M*). Thus, epithelial *Pygo2* is not essential for physiological hair cycle timing, but speeds up HF regeneration in a wound model.

**Epithelial *Pygo2* Is Required for K14-NBC-Induced Anagen Entry and HG Cell Proliferation.** Given the parallels between *Pygo2* expression and active Wnt signaling in the HF (8), we sought to determine if *Pygo2* regulates pathological HF regeneration via

Wnt/ $\beta$ -catenin signaling. Previous work has demonstrated that *K14-NBC* transgenic mice, which express a constitutively nuclear  $\beta$ -catenin in skin keratinocytes, exhibit precocious anagen entry (8). Thus, we generated NBC/SSKO mice (B6/129/CD1 mixed background; B6 < 37%) to determine whether loss of *Pygo2* in skin epithelia could abrogate the effects of excess Wnt/ $\beta$ -catenin signaling. As reported (8), when HFs in WT mice were in second telogen at the age of 50–60 d, most HFs in NBC littermates had progressed to anagen (Fig. 2*A* and *B*). This premature anagen entry was near-completely rescued when *Pygo2* was deleted, as a vast majority of the HFs in NBC/SSKO littermates remained in telogen (Fig. 2*A* and *B*).

Also as expected (8), BrdU<sup>+</sup> and Ki67<sup>+</sup> cells were detected in the HGs of NBC but rarely WT HFs with a telogen morphology (Fig. 2*C–E*). In contrast, loss of *Pygo2* resulted in a significant reduction in the number of proliferative HG cells, as few BrdU<sup>+</sup> or Ki67<sup>+</sup> cells were observed in telogen HFs of NBC/SSKO littermates (Fig. 2*C–E* and Fig. S5*A*). Neither the proliferation nor the number of bulge cells was significantly affected by *Pygo2* loss at the telogen stage (Fig. S5). Thus, *Pygo2* is required for  $\beta$ -catenin-induced activation of EPCs in the HG, and consequently facilitates HF regeneration.

***Pygo2* Facilitates  $\beta$ -Catenin-Mediated Wnt Target Gene Expression but Not Lhx2<sup>+</sup> Cell Expansion in the HG.** To further understand how *Pygo2* regulates  $\beta$ -catenin function in skin, we examined whether Wnt target genes such as *cyclin D1* (*Ccnd1*) or *Lef1* (8, 23) are altered in the absence of *Pygo2*. The levels of *cyclin D1* and *Lef1* transcripts produced by the NBC skin were indeed reduced upon *Pygo2* loss (Fig. 3*A*). Using chromatin immunoprecipitation (ChIP), we found *Pygo2* to co-occupy the *cyclin D1* and *Lef1* promoters with  $\beta$ -catenin in epidermis isolated from NBC mice (Fig. 3*B*). Finally, HFs of P49–50 NBC mice displayed elevated cyclin D1 protein expression in their HGs (8); when *Pygo2* was deleted, this up-regulation was abolished (Fig. 3*C* and *D*). Taken together, these data indicate that *Pygo2* occupancy promotes *cyclin D1* expression in HG cells. Furthermore, compared with nontransgenic controls, the number of Lef1<sup>+</sup> cells

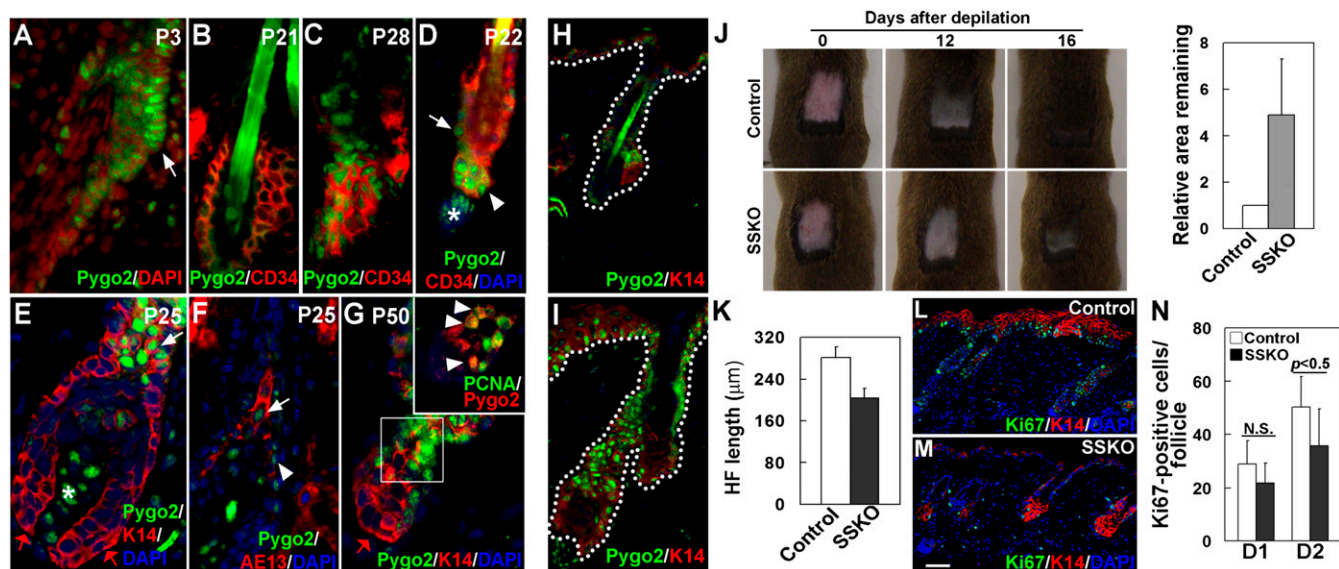


**Fig. 1.** *Pygo2* is dynamically expressed in HF SC/EPCs, and it facilitates depilation-induced hair regeneration. (A–G) Indirect immunofluorescence of HFs at different postnatal (P) ages using the indicated antibodies. DAPI stains the nuclei. White arrows indicate bulge cells in *A* and *D*, K14<sup>+</sup> ORS cells in *E*, and AE13<sup>+</sup> precortex cells in *F*. The red arrow in *E* and *G* indicates matrix cells. White arrowheads indicate HG cells in *D*, IRS cells adjacent to the precortex in *F*, and *Pygo2*<sup>+</sup>/PCNA<sup>+</sup> cells in *G*. White asterisks in *D* and *E* denote *Pygo2*<sup>+</sup> DP cells. Inset in *G* shows an enlarged image of the boxed area. (*H* and *I*) Hair depilation up-regulates *Pygo2* protein. Control (*H*) and depilated (*I*) skin of the same mouse were analyzed 2 d after depilation (D2). (*J*) Loss of *Pygo2* delays postdepilation hair regeneration. For quantitative analysis (*Right*), the area that remained in each mouse ( $n = 5$  for control;  $n = 3$  for SSKO) was measured at D11–16, and that of the control was arbitrarily set to be 1. (*K*) Reduced HF length in depilated SSKO skin at D2 ( $n = 3$ ). (*L–N*) Ki67 staining of control and SSKO skin at D1 and D2. Quantification (*N*) was done for proliferative cells in the HF ( $n = 3$ ). Error bars denote standard deviation (SD). Control genotypes, *Pygo2*<sup>+/+</sup> or *K14-Cre/Pygo2*<sup>+/+</sup>. [Scale bar, 10  $\mu$ m (A–G), 15  $\mu$ m (*H* and *I*), and 45  $\mu$ m (*L* and *M*).]

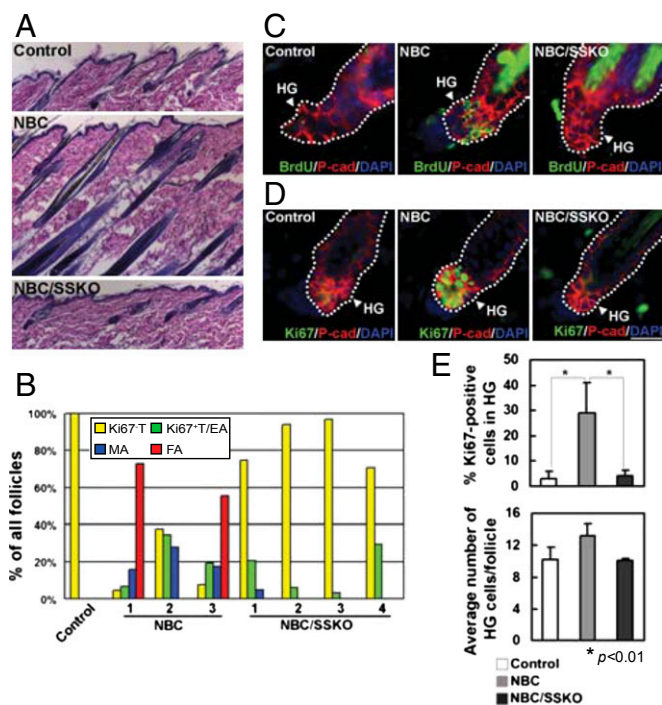


**Fig. 2.** Hair cycle and HG proliferation in control, NBC, and NBC/SSKO mice. (A) H&E analysis of P63 skin ( $n = 2$ ). (B) Quantification of hair cycle distribution in P56 skin. Number indicates individual mouse with the indicated genotypes. EA, early anagen; FA, full anagen; MA, mid anagen; T, telogen. See *SI Materials and Methods* for stage determination. (C and D) Indirect immunofluorescent detection of BrdU<sup>+</sup> (C) and Ki67<sup>+</sup> (D) cells in the HG (P-cadherin<sup>+</sup>). (E) Quantification of Ki67<sup>+</sup> HG cells (Upper) and average number of HG cells per each HF section (Lower) in control ( $n = 4$ ), NBC ( $n = 7$ ), and NBC/SSKO ( $n = 4$ ) mice. Error bars denote SD. Exact genotypes are *Pygo2*<sup>+/f</sup> or *K14-Cre/Pygo2*<sup>+/f</sup> for the control group and *NBC/Pygo2*<sup>+/f</sup> or *NBC/K14-Cre/Pygo2*<sup>+/f</sup> for the NBC group. [Scale bar, 180  $\mu$ m (A) and 20  $\mu$ m (C and D).]

increased by twofold in NBC telogen HF, and this increase was slightly compromised in NBC/SSKO HGs (Fig. 3 C and E).

Given the role of Wnt/ $\beta$ -catenin signaling in bulge SC fate determination (9), we wondered whether *Pygo2* may function with  $\beta$ -catenin to control the size of an HF progenitor pool within the growing HG. *Lhx2* marks embryonic hair germ and adult bulge/HG SC/EPCs (24), whereas *p63* is a “pan” epithelial stem/progenitor cell marker (25). Therefore, we analyzed the number of *Lhx2*<sup>+</sup> cells in reference to *p63*<sup>+</sup> cells to determine whether *Pygo2* was involved in regulating the total cell number within the HG or in controlling HF progenitor cell fate. Compared with the WT, HGs from NBC mice displayed a  $\sim$ twofold increase in the number of *Lhx2*<sup>+</sup> cells (Fig. 3 C and F), similar in extent to the increase in *Lef1*<sup>+</sup> cells. Interestingly, despite a lack of appreciable cell proliferation, HGs from NBC/SSKO mice displayed a similar increase in *Lhx2*<sup>+</sup> cells. The number of HG *p63*<sup>+</sup> cells was not significantly affected by either NBC expression or *Pygo2* loss (Fig. 3 C and G). Thus, it appears that NBC expands *Lhx2*<sup>+</sup> cells in the HG via a mechanism that is independent of proliferation and *Pygo2*.

**$\beta$ -Catenin and *Pygo2* Converge to Induce *p53* Accumulation and Acetylation upon Anagen Entry and in Cultured Keratinocytes.** Because *Pygo2* was required for NBC-induced HG proliferation and cyclin D1 expression, we next investigated whether it functions with  $\beta$ -catenin to control the expression of additional regulators of the cell cycle, such as Rb, *p53*, *p21*, and *p16* (26). Although a difference was not statistically significant, there appeared to be more telogen bulge and HG cells that were positive for Rb phosphorylation at serine 807/811 (P-Rb) in NBC

mice than the WT control (Fig. 4A and Fig. S6A). However, *Pygo2* loss did not exert any detectable effect on the number of P-Rb–positive NBC HG cells. Moreover, no significant difference in the number of *p21*<sup>+</sup> or *p16*<sup>+</sup> HG cells was detected among the three genotypes (Fig. 4A and Fig. S6B). In contrast, the numbers of cells expressing total and, more strikingly, acetylated *p53* [an activated form (27)] in the HG of NBC mice were increased compared with WT, and these increases were abolished in NBC/SSKO mice (Fig. 4A and B and Fig. S6C and D). Thus, forced  $\beta$ -catenin signaling leads to increased levels of total and acetylated *p53* within the HG, and this effect requires *Pygo2*.

The accumulation and activation of *p53* in NBC HG could be molecular events that accompany HF SC activation or simply consequences of abnormally high oncogenic signaling. To address this, we determined if *p53* is activated during T–A transition in a nontransgenic background. Acetylated *p53* was detected in the HG cells at anagen stages I and II, and subsequently in the bulge cells at anagen III of WT mice (Fig. 4C), coinciding exactly with the timing of sequential activation of the HG and bulge cells, respectively (4), as well as with the timing/location of endogenous Wnt signaling activity (9). Acetyl-*p53* was also detected in the regenerating HF 2 d after depilation, and a trend of a decrease of acetyl-*p53*–positive cells was observed when *Pygo2* was deleted (Fig. S6E). Thus, *p53* acetylation also accompanies physiological and depilation-induced HF SC/EPC activation.

To dissect keratinocyte-intrinsic effects of  $\beta$ -catenin and *Pygo2* on *p53* expression, we turned to HaCaT keratinocytes. Overexpression of NBC in HaCaT cells led to the nuclear accumulation of total, acetyl (382)-, as well as serine 15-phosphorylated *p53* proteins (Fig. 4D). Western blot analysis revealed that the increase in the level of acetyl-*p53* is the most pronounced of all (Fig. 4E). In contrast, no change in the level of *p53* (*Trp53*) transcripts was observed (Fig. S7A). Importantly, siRNA-mediated depletion of *Pygo2* resulted in a reduction of acetyl-*p53* and, to a lesser extent, total *p53* in HaCaT

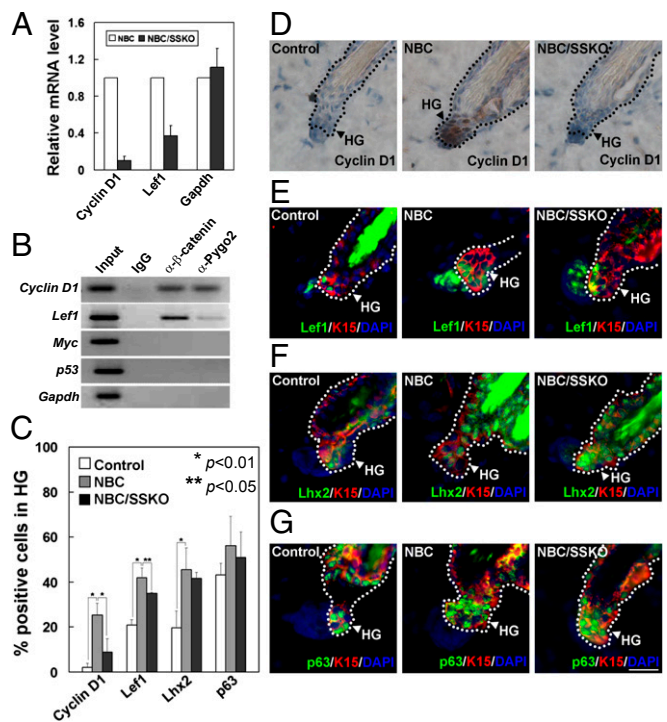


**Fig. 3.** Expression of Wnt targets and stem/progenitor cell markers in telogen follicles of control, NBC, and NBC/SSKO mice. (A) RT-quantitative PCR analysis. (B) ChIP analysis using epidermis of NBC mice. (C) Quantitative analysis of immunostaining results (D–G) using the indicated antibodies. Arrowhead indicates the K15<sup>+</sup> HG field. Error bars denote SD. See Fig. 2 legends for control genotypes. [Scale bar, 20  $\mu$ m (D–G).]

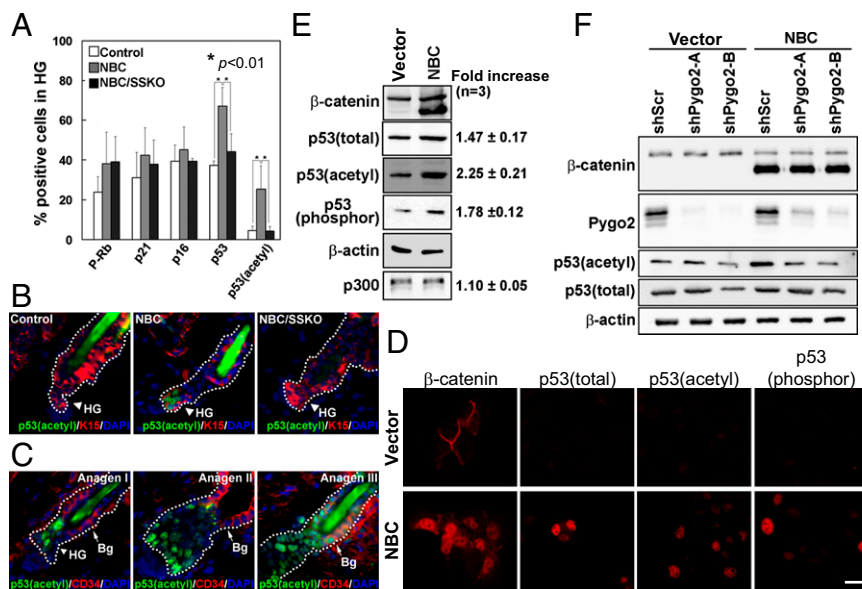


**Fig. 4.** Pygo2-dependent p53 activation upon  $\beta$ -catenin overexpression and T–A transition. (A) Quantitative analysis for cell-cycle regulators in telogen HF from control, NBC, and NBC/SSKO mice. Error bars denote SD. (B) Representative images showing acetyl-p53 immunostaining results. Arrowhead and arrow indicate  $K15^+$  HG and  $CD34^+$  bulge cells, respectively. See Fig. 2 legends for control genotypes. (C) Emergence of acetyl-p53 during normal T–A transition. (D and E) Indirect immunofluorescence (D) and Western blotting (E) of various forms of p53 protein in HaCaT cells. Values on the right indicate  $\beta$ -catenin-induced fold change. (F) Effect of Pygo2 depletion on p53 protein. [Scale bar, 20  $\mu$ m (B and C) and 10  $\mu$ m (D).]

cells, especially when  $\beta$ -catenin was overexpressed (Fig. 4F). These molecular data show that  $\beta$ -catenin and Pygo2 converge to post-transcriptionally regulate p53, particularly at the level of acetylation, in epidermal keratinocytes. Collectively, our findings identify p53 activation as a prominent downstream event of the  $\beta$ -catenin/Pygo2 pathway in HF SC/EPC activation.

**p53 Involvement in  $\beta$ -Catenin Function Appears Complex, but Pygo2 Is Required for NBC-Induced Follicular Hyperplasia.** To explore whether p53 mediates  $\beta$ -catenin action in HF SC activation, we bred homozygous *p53* null alleles into the NBC mice, with the resulting strain background being B6-enriched (B6/CD1; B6 = 75%) Compared with NBC control (*p53*<sup>+/+</sup> or *p53*<sup>+/-</sup>) littermates, 5-mo-old NBC/*p53*<sup>-/-</sup> mice (*n* = 3) showed apparently less severe skin overgrowths and less elaborate trichofolliculoma-like structures (Fig. S8A). We also examined younger mice to ask whether *p53* loss affects NBC-induced anagen entry. Unfortunately, the B6-enriched strain background significantly decreased the penetrance of precocious anagen entry in NBC mice: At the ages (76–81 d) examined, three out of 15 (20%) NBC or NBC/*p53*<sup>+/-</sup> mice had progressed prematurely into anagen (Fig. S8B). Only one out of 11 (9%) NBC/*p53*<sup>-/-</sup> littermates showed anagen entry. Enriching for CD1 strain background was able to increase the penetrance; however, NBC control and NBC/*p53*<sup>-/-</sup> littermates now showed comparable frequencies of anagen progression (Fig. S8B). We next depilated *p53*<sup>-/-</sup> mice at telogen, but again did not detect any obvious difference in their hair regeneration and anagen progression from control littermates (Fig. S8C and D). Therefore, although p53 is present and activated upon HF SC/EPC activation, our studies fail to reveal strong evidence for its positive involvement in anagen entry or progression.

Finally, we returned to the NBC/Pygo2 SSKO model to ask whether Pygo2 is important for NBC-induced skin hyperplasia and tumorigenesis. At the age of 6–8 mo, all NBC mice in the B6/129/CD1 mixed background analyzed (*n* = 28) showed clearly visible paw overgrowths and most showed mouth and ear overgrowths, whereas none of the control mice (*n* = 17) did (Fig. 5A). Remarkably, 12 out of 15 age-matched NBC/SSKO mice completely lacked these abnormal growths, whereas the remaining three developed some paw overgrowths but to a much lesser extent (Fig. 5A). Rescue was equally evident at the histological level: the NBC-induced abnormal HFs associated with trichofolliculoma-like structures were near-completely abolished in SSKO mice (Fig. 5B). Moreover, skin epithelium including the IFE from NBC mice

abundantly expressed K6, a hyperproliferation marker, the expression of which is normally restricted to the companion layer of the HF (28), whereas the number of  $K6^+$  cells was significantly reduced in both IFE and HFs from the NBC/SSKO mice (Fig. 5C). As expected (10, 29), NBC mice developed pilomatricomas at older ages at low penetrance (Fig. S9). Despite the reduction in hyperplasia, 27% of the NBC/SSKO mice (*n* = 26) produced pilomatricomas by the age of 8 mo, compared with 15% of age-matched NBC mice (*n* = 39) (Fig. S9). Collectively, these results underscore a requirement for Pygo2 in NBC-induced follicular hyperplasia but not tumorigenesis.

## Discussion

Our work provides convincing evidence for a functional involvement of chromatin effector Pygo2 in  $\beta$ -catenin-induced anagen entry and follicular hyperplasia (Fig. 6). A cell-autonomous, facilitative role for Pygo2 in  $\beta$ -catenin-induced HG activation/proliferation is consistent with previous studies identifying Pygo proteins as Wnt coactivators in flies and cultured cells. As such, our findings suggest that the specific action of Wnt/ $\beta$ -catenin in precociously activated HF SC/EPCs may entail chromatin activation, particularly at specific Wnt target loci such as *cyclin D1* and *Lef1*.

Our work also supports the emerging view that epigenetic mechanisms are important for HF SC activation (30, 31). Among the chromatin factors that regulate HF SC behaviors *in vivo* is Jarid2, a component of the polycomb repressive complex 2 (PRC2) that facilitates PRC2 recruitment to target loci and that regulates PRC2 histone H3 lysine 27 (H3K27) methyltransferase activity (31). Loss of Jarid2 does not affect the number of bulge SCs, but delays the proliferation of HG and the more lineage-restricted progenitor cells, consequently delaying anagen entry. Brg1, a catalytic subunit of the switch/sucrose nonfermentable (SWI/SNF) chromatin remodeling complex, maintains the bulge SCs and acts downstream of sonic hedgehog signaling to fuel hair growth (32). Together, these and our findings highlight the importance of tuning histone modifications, particularly the H3K27me3 and H3K4me3 marks, as well as ATP-dependent chromatin remodeling in HF SC biology.

Interestingly, a requirement for Pygo2 is only manifest during depilation- or  $\beta$ -catenin-induced anagen entry, but not physiological T–A transition. Although the level of *Pygo1* transcripts was not altered in the SSKO skin (Fig. S3B), it remains possible that Pygo1 acts redundantly with Pygo2 during the native hair cycle. Regardless, however, Pygo2 function is indispensable under pathological conditions when the demand for SC activation

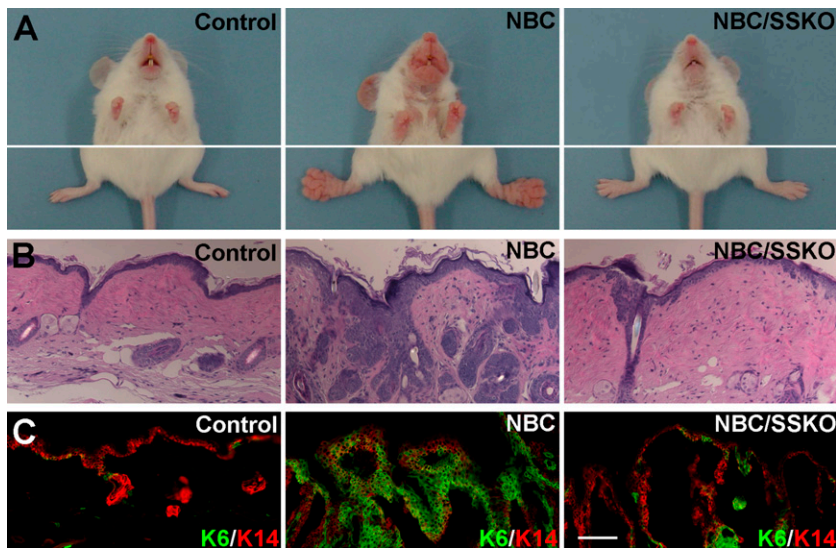


**Fig. 5.** Loss of Pygo2 suppresses NBC-induced trichofolliculoma formation. (A–C) Overall appearance (A), paw skin histology (H&E) (B), and K6/K14 immunostaining (C) of control (*Pygo2*<sup>+/f</sup>), NBC (also *Pygo2*<sup>+/f</sup>), and NBC/SSKO mice. [Scale bar, 100  $\mu$ m (B and C).]

is high. Whether Pygo2 is required for other diseased skin conditions where Wnt/ $\beta$ -catenin is aberrantly active (33) is worthy of future investigation.

*Pygo2* null mice display reduced HF density during embryogenesis and sparse hair coats as adults, but epithelial deletion of *Pygo2* does not phenocopy these. This implies that Pygo2 produced by nonepithelial cell types is functionally important for HF morphogenesis. Recently, neural crest-derived Pygo2 has been shown to promote HF development (34). Moreover, the strong expression of Pygo2 in DP of embryonic and adult HFs raises the possibility that DP-derived Pygo2 may participate in embryonic HF development and postnatal cycling.

Why does Pygo2 loss affect NBC-induced trichofolliculoma-like hyperplasia but not pilomatricoma formation? Follicular hyperplasia possibly arises from aberrantly activated HF EPCs and/or IFE cells that have adopted HF stem-like features, because (i) the abnormal HFs in NBC mice express HG but not bulge markers (4) and (ii) anagen entry and follicular hyperplasia in NBC mice are jointly impacted by loss of Pygo2. On the other hand, pilomatricoma arises from the more differentiated, highly proliferative matrix cells (29). Our data show that a hyperplastic follicular environment is not a prerequisite for pilomatricoma formation. A differential requirement for Pygo2 in follicular hyperplasia versus tumorigenesis may root from distinct Pygo2 roles in the two different cell-of-origin populations, such that Pygo2 regulates the proliferation of cells with SC/EPC characteristics, but not late progenitor cells. Moreover, in sharp contrast to the pilomatricoma phenotype, *Pygo2* deletion delayed the initiation of Wnt-induced mammary adenocarcinoma (35), suggesting a tumor-type-specific Pygo2 dependence.

Tumor suppressor protein p53 has been shown to facilitate the regression of actively growing HFs by promoting apoptosis (36). Thus, the accumulation and activation of p53 immediately upon HF SC/EPC activation are rather unexpected. These events occur in a manner that does not coincide exactly with the expression of p21, a well-known p53 target (Fig. 3D), or apoptosis (Fig. S6F). We also note that skin from *p53* null mice showed a trend of up-regulation in *p63* expression during T–A transition (Fig. S7C). *p53* transcription is up-regulated when unstressed cells in culture transition from G0/G1 to S phase, and recent studies suggest this to be important for a rapid p53-mediated response to DNA damage before exiting the S phase (37). Although we cannot formally exclude the possibility that p53 fine-tunes anagen entry or progression, it is more likely that p53 facilitates pathological regeneration as a guardian of genomic integrity in the activated SC/EPC cells by eliminating cells that have sustained damages or replication errors (Fig. 6). Although addressing these issues lies

outside the scope of this study, several reports support the latter notion: p53 protein is stabilized in the skin epithelium following irradiation and loss of *Brca1* (38, 39), and *p53* ablation in mice where *Atr* is deleted locally in skin causes a severe delay in depilation-induced HF regeneration due to accumulation of too many damaged cells (40). Most importantly, our results demonstrate that (i) the quiescence-to-proliferation transition of HF SC/EPCs in vivo resembles cultured cells that receive mitogenic stimuli in mounting a p53 response and (ii)  $\beta$ -catenin and Pygo2 act together to induce this response in epidermal stem/progenitor cells.

Overexpressed or stabilized  $\beta$ -catenin in fibroblasts results in p53 accumulation via transcriptionally inducing alternate reading frame (ARF) of the *INK4a/ARF* locus, which sequesters Mdm2 away from targeting p53 for degradation (41). How is the p53 pathway activated in skin epithelial cells? Our data do not support transcriptional regulation to be the primary mechanism because (i) RT-PCR revealed a minimal increase in *p53* transcripts during physiological T–A transition and no change upon  $\beta$ -catenin overexpression (Fig. S7A and B), in sharp contrast to the remarkable up-regulation of total/acetylated p53

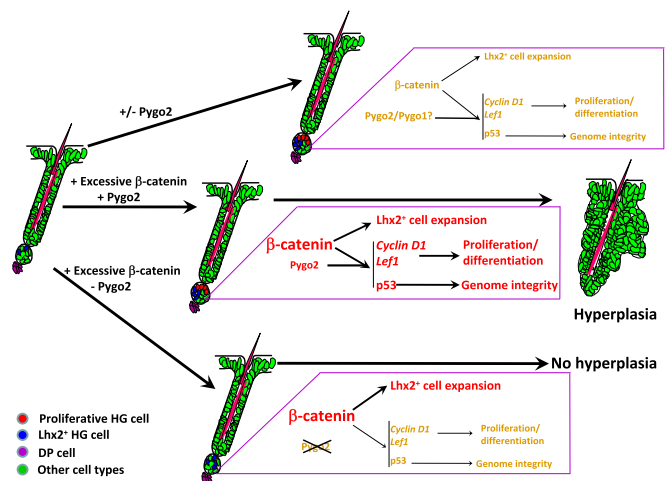


**Fig. 6.** Model of  $\beta$ -catenin and Pygo2 functions in HG activation and follicular hyperplasia. Pygo2 mediates NBC stimulation of HG cell proliferation, but not Lhx2<sup>+</sup> cell expansion. p53 acts downstream of  $\beta$ -catenin and Pygo2 to ensure genome integrity.

protein during both physiological and  $\beta$ -catenin-stimulated T-A transition (Fig. 4), and (ii) our ChIP assay failed to reveal  $\beta$ -catenin and Pygo2 binding to the p53 promoter (Fig. 3). Instead, the effects of  $\beta$ -catenin and Pygo2 are the most striking at the level of p53 acetylation. The protein level of p300, an acetyltransferase that acetylates p53 at lysine 382, was not altered by  $\beta$ -catenin overexpression (Fig. 4E). Moreover, our coimmunoprecipitation experiment did not detect any physical association between p53 and the  $\beta$ -catenin/Pygo2 complex (Fig. S7D). Thus, the jury is still out as to how  $\beta$ -catenin and Pygo2 promote p53 acetylation in epidermal cells.

## Materials and Methods

**Mice.** *Pygo2*<sup>-/-</sup> and SSKO mice (B6/129 mixed background or congenic B6 background) were generated as previously described (15, 21). NBC (CD1 background) mice were a gift of E. Fuchs (The Rockefeller University, New York). *p53*<sup>+/-</sup> mice (congenic B6 background) were purchased from the Jackson Laboratory.

**Morphology, BrdU Labeling, and Immunostaining.** For histological analysis, mouse back skin (identical locations between control and mutants) was fixed in 4% (wt/vol) paraformaldehyde in PBS, embedded in paraffin, sectioned, and stained with hematoxylin and eosin (H&E).

BrdU (Sigma-Aldrich) labeling experiments were performed as described (42). Mice 49 d old (P49) were intraperitoneally injected once with BrdU (50  $\mu$ g/g) and analyzed 24 h later. BrdU incorporation was detected using an anti-mouse BrdU antibody (Abcam; ab6326). To determine the proliferative index in HG, slides were double-stained for P-cadherin, and the percent of BrdU<sup>+</sup> cells per P-cadherin<sup>+</sup> cells within the HG compartment was determined.

- Beck B, Blanpain C (2012) Mechanisms regulating epidermal stem cells. *EMBO J* 31(9):2067–2075.
- Fuchs E (2009) The tortoise and the hair: Slow-cycling cells in the stem cell race. *Cell* 137(5):811–819.
- Woo WM, Oro AE (2011) SnapShot: Hair follicle stem cells. *Cell* 146(2):334–334.e332.
- Greco V, et al. (2009) A two-step mechanism for stem cell activation during hair regeneration. *Cell Stem Cell* 4(2):155–169.
- Reya T, Clevers H (2005) Wnt signalling in stem cells and cancer. *Nature* 434(7035):843–850.
- Choi YS, et al. (2013) Distinct functions for Wnt/ $\beta$ -catenin in hair follicle stem cell proliferation and survival and interfollicular epidermal homeostasis. *Cell Stem Cell* 13(6):720–733.
- Huelsken J, Vogel R, Erdmann B, Cotsarelis G, Birchmeier W (2001)  $\beta$ -catenin controls hair follicle morphogenesis and stem cell differentiation in the skin. *Cell* 105(4):533–545.
- Lowry WE, et al. (2005) Defining the impact of  $\beta$ -catenin/Tcf transactivation on epithelial stem cells. *Genes Dev* 19(13):1596–1611.
- Lien WH, et al. (2014) In vivo transcriptional governance of hair follicle stem cells by canonical Wnt regulators. *Nat Cell Biol* 16(2):179–190.
- Gat U, DasGupta R, Degenstein L, Fuchs E (1998) De novo hair follicle morphogenesis and hair tumors in mice expressing a truncated  $\beta$ -catenin in skin. *Cell* 95(5):605–614.
- Lo Celso C, Prowse DM, Watt FM (2004) Transient activation of  $\beta$ -catenin signalling in adult mouse epidermis is sufficient to induce new hair follicles but continuous activation is required to maintain hair follicle tumours. *Development* 131(8):1787–1799.
- Van Mater D, Kolligs FT, Dlugosz AA, Fearon ER (2003) Transient activation of  $\beta$ -catenin signaling in cutaneous keratinocytes is sufficient to trigger the active growth phase of the hair cycle in mice. *Genes Dev* 17(10):1219–1224.
- Jessen S, Gu B, Dai X (2008) Pygopus and the Wnt signaling pathway: A diverse set of connections. *BioEssays* 30(5):448–456.
- Fiedler M, et al. (2008) Decoding of methylated histone H3 tail by the Pygo-BCL9 Wnt signaling complex. *Mol Cell* 30(4):507–518.
- Gu B, et al. (2009) Pygo2 expands mammary progenitor cells by facilitating histone H3 K4 methylation. *J Cell Biol* 185(5):811–826.
- Andrews PG, He Z, Popadiuk C, Kao KR (2009) The transcriptional activity of Pygopus is enhanced by its interaction with cAMP-response-element-binding protein (CREB)-binding protein. *Biochem J* 422(3):493–501.
- Chen J, et al. (2010) Pygo2 associates with MLL2 histone methyltransferase and GCN5 histone acetyltransferase complexes to augment Wnt target gene expression and breast cancer stem-like cell expansion. *Mol Cell Biol* 30(24):5621–5635.
- Gu B, Watanabe K, Dai X (2012) Pygo2 regulates histone gene expression and H3 K56 acetylation in human mammary epithelial cells. *Cell Cycle* 11(1):79–87.
- Nair M, et al. (2008) Nuclear regulator Pygo2 controls spermiogenesis and histone H3 acetylation. *Dev Biol* 320(2):446–455.
- Gu B, Watanabe K, Sun P, Fallahi M, Dai X (2013) Chromatin effector Pygo2 mediates Wnt-notch crosstalk to suppress luminal/alveolar potential of mammary stem and basal cells. *Cell Stem Cell* 13(1):48–61.
- Coller HA (2007) What's taking so long? S-phase entry from quiescence versus proliferation. *Nat Rev Mol Cell Biol* 8(8):667–670.
- Ito M, Kizawa K, Toyoda M, Morohashi M (2002) Label-retaining cells in the bulge region are directed to cell death after plucking, followed by healing from the surviving hair germ. *J Invest Dermatol* 119(6):1310–1316.
- Hovanes K, et al. (2001)  $\beta$ -catenin-sensitive isoforms of lymphoid enhancer factor-1 are selectively expressed in colon cancer. *Nat Genet* 28(1):53–57.
- Rhee H, Polak L, Fuchs E (2006) Lhx2 maintains stem cell character in hair follicles. *Science* 312(5782):1946–1949.
- Senoo M, Pinto F, Crum CP, McKeon F (2007) p63 is essential for the proliferative potential of stem cells in stratified epithelia. *Cell* 129(3):523–536.
- Johnson DG, Walker CL (1999) Cyclins and cell cycle checkpoints. *Annu Rev Pharmacol Toxicol* 39:295–312.
- Sakaguchi K, et al. (1998) DNA damage activates p53 through a phosphorylation-acetylation cascade. *Genes Dev* 12(18):2831–2841.
- Rothnagel JA, et al. (1999) The mouse keratin 6 isoforms are differentially expressed in the hair follicle, footpad, tongue and activated epidermis. *Differentiation* 65(2):119–130.
- Chan EF, Gat U, McNiff JM, Fuchs E (1999) A common human skin tumour is caused by activating mutations in  $\beta$ -catenin. *Nat Genet* 21(4):410–413.
- Lien WH, et al. (2011) Genome-wide maps of histone modifications unwind in vivo chromatin states of the hair follicle lineage. *Cell Stem Cell* 9(3):219–232.
- Mejta S, et al. (2011) Jarid2 regulates mouse epidermal stem cell activation and differentiation. *EMBO J* 30(17):3635–3646.
- Xiong Y, et al. (2013) Brg1 governs a positive feedback circuit in the hair follicle for tissue regeneration and repair. *Dev Cell* 25(2):169–181.
- Malanchi I, et al. (2008) Cutaneous cancer stem cell maintenance is dependent on  $\beta$ -catenin signalling. *Nature* 452(7187):650–653.
- Narytnyk A, Gillinder K, Verdon B, Clewes O, Sieber-Blum M (2013) Neural crest stem cell-specific deletion of the Pygopus2 gene modulates hair follicle development. *Stem Cell Rev* 10(1):60–68.
- Watanabe K, Fallahi M, Dai X (2014) Chromatin effector Pygo2 regulates mammary tumor initiation and heterogeneity in MMTV-Wnt1 mice. *Oncogene* 33(5):632–642.
- Botchkarev VA, et al. (2001) p53 involvement in the control of murine hair follicle regression. *Am J Pathol* 158(6):1913–1919.
- Reisman D, Takahashi P, Polson A, Boggs K (2012) Transcriptional regulation of the p53 tumor suppressor gene in S-phase of the cell-cycle and the cellular response to DNA damage. *Biochem Res Int* 2012:808934.
- Sotiropoulou PA, et al. (2010) Bcl-2 and accelerated DNA repair mediates resistance of hair follicle bulge stem cells to DNA-damage-induced cell death. *Nat Cell Biol* 12(6):572–582.
- Sotiropoulou PA, et al. (2013) BRCA1 deficiency in skin epidermis leads to selective loss of hair follicle stem cells and their progeny. *Genes Dev* 27(1):39–51.
- Ruzankina Y, et al. (2009) Tissue regenerative delays and synthetic lethality in adult mice after combined deletion of Atr and Trp53. *Nat Genet* 41(10):1144–1149.
- Damalas A, Kahan S, Shtutman M, Ben-Ze'ev A, Oren M (2001) Deregulated  $\beta$ -catenin induces a p53- and ARF-dependent growth arrest and cooperates with Ras in transformation. *EMBO J* 20(17):4912–4922.
- Braun KM, et al. (2003) Manipulation of stem cell proliferation and lineage commitment: Visualisation of label-retaining cells in whole mounts of mouse epidermis. *Development* 130(21):5241–5255.
- Li B, et al. (2007) Developmental phenotypes and reduced Wnt signaling in mice deficient for pygopus 2. *Genesis* 45(5):318–325.

For indirect immunofluorescence, mouse back skin was freshly frozen in optimal cutting temperature compound (OCT) (Tissue Tek), sectioned (6–8  $\mu$ m), and staining was performed using the appropriate antibodies. Immunohistochemical detection was performed with paraformaldehyde-fixed OCT sections, using Vector ABC (Vector Laboratories; PK-6100) and DAB (DAKO; K3468) kits according to the manufacturers' recommendations. Antigen retrieval was performed by incubating slides in 0.01 M citrate buffer (pH 6.0) in a microwave at full power for 3–5 min.

**ChIP Analysis.** Epidermis from NBC mice (three mice per experiment) was isolated using 2.5 mg/mL Dispase (Stem Cell Technologies; 07913) and directly fixed with 1% formaldehyde. After washing, the chromatin was sheared using a Bioruptor (Diagenode) and subjected to immunoprecipitation with control IgG (Santa Cruz Biotechnology; sc-2027), anti-Pygo2 (43), or anti- $\beta$ -catenin (Santa Cruz Biotechnology; sc-7199) antibody. Immunoprecipitated DNA was purified after reverse cross-linking, and ChIP-PCR was performed using the indicated primers.

Additional details for the above procedures as well as procedures for cell culture, siRNA knockdown, Western blot, RNA isolation, and RT-PCR are described in *SI Materials and Methods*.

**ACKNOWLEDGMENTS.** We thank Elaine Fuchs and Sarah Millar for NBC and *K14-Cre* mice, respectively, and the Optical Biology Center for expert service. This work was supported by National Institutes of Health (NIH) Grants R01-AR47320, R01-GM083089, and K02-AR51482 (to X.D.) and National Science Foundation Grant DMS-116162 (to Qing Nie and X.D.). B.L. was supported as a predoctoral trainee on NIH Training Grants T32HD060555 and T32CA113265. V.H. is a Pew Scholar in Biomedical Research and is supported by the NIH (R01-AR060295) and Connecticut Innovations (12-SCB-YALE-01 and 12-SCA-YALE-09).